

# Chromatic discrimination of natural objects

**Thorsten Hansen**

Department of Psychology, Justus-Liebig-University,  
Giessen, Germany



**Martin Giesel**

Department of Psychology, Justus-Liebig-University,  
Giessen, Germany



**Karl R. Gegenfurtner**

Department of Psychology, Justus-Liebig-University,  
Giessen, Germany



Studies of chromatic discrimination are typically based on homogeneously colored patches. Surfaces of natural objects, however, cannot be characterized by a single color. Instead, they have a chromatic texture, that is, a distribution of different chromaticities. Here we study chromatic discrimination for natural images and synthetic stimuli with a distribution of different chromaticities under various states of adaptation. Discrimination was measured at the adaptation point, where the mean chromaticity of the test stimuli was the same as the chromaticity of the adapting background, and away from the adaptation point. At the adaptation point, discrimination for natural objects resulted in threshold contours that were selectively elongated in a direction of color space matching the chromatic variation of the colors within the natural object. Similar effects occurred for synthetic stimuli. Away from the adaptation point, discrimination thresholds increased and threshold ellipses were elongated along the contrast axis connecting adapting color and test color. Away from the adaptation point, no significant differences between the different stimulus classes were found. The effect of the chromatic texture on discrimination seemed to be masked by the overall increase in discrimination thresholds. Our results show that discrimination of chromatic textures, either synthetic or natural, differs from that of simple uniform patches when the chromatic variation is centered at the adaptation point.

Keywords: chromatic discrimination, natural objects, chromatic textures, chromatic distribution, spatial frequency

Citation: Hansen, T., Giesel, M., & Gegenfurtner, K. R. (2008). Chromatic discrimination of natural objects. *Journal of Vision*, 8(1):2, 1–19, <http://journalofvision.org/8/1/2/>, doi:10.1167/8.1.2.

## Introduction

The study of chromatic discrimination has a long history (MacAdam, 1942; Schrödinger, 1920; Stiles, 1959; von Helmholtz, 1867; Wright, 1941). It has been in the focus of interest not only to elucidate the mechanisms underlying color vision, but also to predict whether two colors can be discriminated by an average observer or not. For a long time, the data set collected by MacAdam (1942) has guided the effort to find equations for an easy, straightforward calculation of color differences. MacAdam measured chromatic discrimination based on the standard deviation of color matches. In his study, observers viewed a bipartite field. The color of one half-field was fixed and defined the test or the reference color. The color of the other half-field had to be adjusted along one of several lines defined in the 1931 CIE chromaticity diagram until it matched the test color. Discrimination contours were then determined based on the variability of the matches along these lines. The contours derived by MacAdam were elliptical and became known as “MacAdam ellipses.” MacAdam measured 25 of such ellipses for test colors sampling the whole CIE chromaticity diagram. A detailed mathematical analysis of

the ellipses revealed that no geometric transformation exists that simultaneously renders all ellipses into circles, which is a prerequisite for a uniform color space (Brown, 1957; Brown & MacAdam, 1949; MacAdam, 1944; Wyszecki & Fielder, 1971a, 1971b). Nevertheless, numerous attempts have been made in the past to find transformations that might roughly approximate a uniform color space (Godlove, 1952; Huertas, Melgosa, & Oleari, 2006; Moon & Spencer, 1943; Newhall, Nickerson, & Judd, 1943; Saunderson & Milner, 1944, 1946; Wyszecki, 1963). The most prominent and most widely used of these transformations were defined in 1978—more than 35 years after MacAdam’s seminal study—as the CIE Lab and the CIE Luv color spaces (CIE, 1978). Since then, more complex color appearance models have been recommended by the CIE such as the CIECAM97s (CIE, 1998; Fairchild, 1998), and uniform color spaces have been proposed based on the CIECAM02 color appearance model (CIE, 2004; Luo, Cui, & Li, 2006; Moroney, et al., 2002).

More recently, several groups have pointed out that adaptation contributes significantly to the complicated pattern of results obtained by MacAdam (1942). In MacAdam’s paradigm, the observer looked at the test color for extended periods while producing the required

match. Therefore, the state of adaptation was fully determined by the test color, and as a result, each measurement for each test color was made under a different state of adaptation. Recent studies have tried to decouple chromatic discrimination at a particular test color from the state of adaptation (Hillis & Brainard, 2005; Kawamoto, Inamura, & Shioiri, 2003; Kiener, 1997; Krauskopf & Gegenfurtner, 1992; Loomis & Berger, 1979; Miyahara, Smith, & Pokorny, 1993; Rinner & Gegenfurtner, 2000; Shapiro, Beere, & Zaidi, 2001, 2003; Shapiro & Zaidi, 1992; Smith & Pokorny, 1996; Smith, Pokorny, & Sun, 2000; Zaidi, Shapiro, & Hood, 1992; Zele, Smith, & Pokorny, 2006). In these studies, the state of adaptation is typically determined by a constant background of a certain color. The test stimuli are then presented on the adapting background only briefly, not to disturb the state of adaptation. A common result of these studies is that the discrimination thresholds for a fixed test color differ considerably with the state of adaptation. To a first approximation, the difference between adapting color and comparison color determines discriminability. An analysis of MacAdam's data by LeGrand (1968) revealed that some directions of color space seem to play a special role (Boynton & Kambe, 1980; MacLeod & Boynton, 1979), and these now seem to be the "cardinal directions of color space" (Krauskopf, Williams, & Heeley, 1982). These cardinal directions of color space correspond to independent mechanisms whose neuronal substrate originates in the cone-opponent cells in the retina and the lateral geniculate nucleus (Derrington, Krauskopf, & Lennie, 1984). Krauskopf and Gegenfurtner (1992) measured chromatic discrimination in the isoluminant plane of the DKL color space under rigorously controlled adaptation conditions. Along each cardinal line, increasing the difference between adapting and standard color increased thresholds for detecting differences in the same cardinal direction, just as predicted by Weber's Law. At the same time, thresholds for differences in the other cardinal directions were unaffected. Unfortunately, if both cardinal mechanisms were activated, the pattern of color difference thresholds was still rather complex (Krauskopf & Gegenfurtner, 1992).

Controlling for the state of chromatic adaptation was a big step forward in understanding chromatic discrimination. However, the typical experimental situations investigated still differ considerably from those in our natural environment. Rather than the color of uniform spots of light, we usually judge the color of objects on a variegated background. Moreover, in natural scenes, both objects and backgrounds do not consist of a single color but are characterized by a whole distribution of colors that vary systematically in chromaticity. It has been shown that color sensitivity and appearance is influenced by adaptation to the color distribution of natural images (Webster & Mollon, 1997). Few studies have investigated chromatic discrimination for stimuli that have a chromatic distribution. In one of these, Zaidi, Spehar, and DeBonet (1998) showed that adaptation to a textured

background influences subsequent chromatic discrimination of homogeneous colors. In the other, te Pas and Koenderink (2004) investigated discrimination thresholds for textured stimuli that varied along different dimensions in RGB color space. The different chromatic textures were chosen to model changes due to shading, specular reflectance, or material. They found elevated discrimination thresholds for the chromatic textures compared with those for uniform colors.

Here we studied chromatic discrimination for digitized photographs of natural fruit and vegetable objects. These objects were chosen because of their ecological validity, easy recognition, and significance. The ability to discriminate ripe fruits from foliage is one of the benefits of color vision and may have played a decisive role in the evolution of trichromacy (e.g., Sumner & Mollon, 2000; Walls, 1942). As demonstrated by te Pas and Koenderink (2004) and Zaidi et al. (1998), chromatic discrimination might be influenced by the chromatic distributions of the chosen objects. Further, chromatic discrimination might also be affected by the familiarity of these objects, all of which have a typical or a memory color associated with them. In particular, Hansen, Olkkonen, Walter, and Gegenfurtner (2006) have shown that the appearance of natural objects is influenced by memory color. In other words, previous knowledge of the chromatic properties of these objects modifies how they are perceived. A similar effect might also influence chromatic discrimination. To disentangle the potential contributions of low-level and high-level effects, we paralleled the discrimination experiments with natural objects by experiments using synthetic chromatic textures. The synthetic textures were chosen to resemble the chromatic and the spatial properties of the natural objects. We find that at the adaptation point, the distribution of chromaticities in natural objects produces a specific increase in discrimination threshold along the axis of maximal chromatic variation. A similar effect occurs for the synthetic textures, suggesting that the increase in discrimination threshold can be attributed to low-level features alone, namely, the chromatic distribution and the spatial frequency content of the stimulus.

## Methods

### Apparatus

The software for stimulus presentation was programmed in C using the SDL library. The stimuli were displayed on a SONY GDM-20se II color CRT monitor. The monitor resolution was set to  $1,280 \times 1,024$  pixels with a refresh rate of 120 Hz noninterlaced. The monitor was controlled by a PC with a color graphics card with 8-bit intensity resolution for each of the three monitor primaries. The nonlinear relationship between voltage

output and luminance was linearized by a color look-up table for each primary. To generate the three RGB look-up tables, we measured the luminance of each phosphor at various voltage levels using a Graseby Optronics Model 307 radiometer with a model 265 photometric filter, and a smooth function was used to interpolate between the measured data. The spectrum of each of the three primaries at its maximum intensity was measured with a Photo Research PR 650 spectroradiometer. The obtained spectra were then multiplied with the Judd-revised CIE 1931 color matching functions (Judd, 1951; Wyszecki and Stiles, 1982) to derive CIE  $xyY$  coordinates of the monitor phosphors. The  $xyY$  coordinates of the monitor primaries at maximum intensity are given by  $R = (0.613, 0.349, 20.289)$ ,  $G = (0.283, 0.605, 64.055)$ , and  $B = (0.157, 0.071, 8.631)$ . The  $xyY$  coordinates were then used to convert between RGB and DKL color space.

## Color space

All stimuli were described in the isoluminant plane of the DKL color space (Derrington et al., 1984; Krauskopf et al., 1982). The DKL color space is a second stage cone-opponent color space, which reflects the preferences of retinal ganglion cells and LGN neurons. It is spanned by an achromatic luminance axis, the  $L + M$  axis, and two chromatic axes, the  $L - M$  axis, and  $S - (L + M)$  axis. The

two chromatic axes define an isoluminant plane. These three so-called cardinal axes intersect at the white point. The  $L + M$  axis is determined by the sum of the signals generated by the long wavelength cones (L-cones) and the middle wavelength cones (M-cones). The  $L - M$  axis is determined by the differences in the signals as generated by the L-cones and the M-cones. Along the  $L - M$  axis, the L- and M-cone excitations covary at a constant sum, while the short wavelength cone (S-cone) excitation does not change. Colors along the  $L - M$  axis vary between reddish and bluish-greenish. The  $S - (L + M)$  axis is determined by the difference in the signals generated by the S-cones and the sum of the L- and M-cones. Along the  $S - (L + M)$  axis, only the excitation of the S-cones changes and colors vary between yellow-greenish and purple. Within the isoluminant plane, colors are commonly defined by polar coordinates of azimuth and amplitude. The azimuth defines the chromatic direction and can be related to hue changes. The azimuth or chromatic direction is  $0^\circ$  for positive excursions along the  $L - M$  axis and ranges in a counterclockwise direction from  $0^\circ$  to  $360^\circ$ . The amplitude is given by the distance from the white point at the origin and can be related to saturation changes. The axes of the DKL color space were scaled from  $-1$  to  $1$ , where  $\pm 1$  corresponds to the maximum contrast achievable for the particular axis on the monitor used. The relationship between these coordinates and the device-independent coordinates ( $r, b$ ) as suggested by MacLeod and Boynton

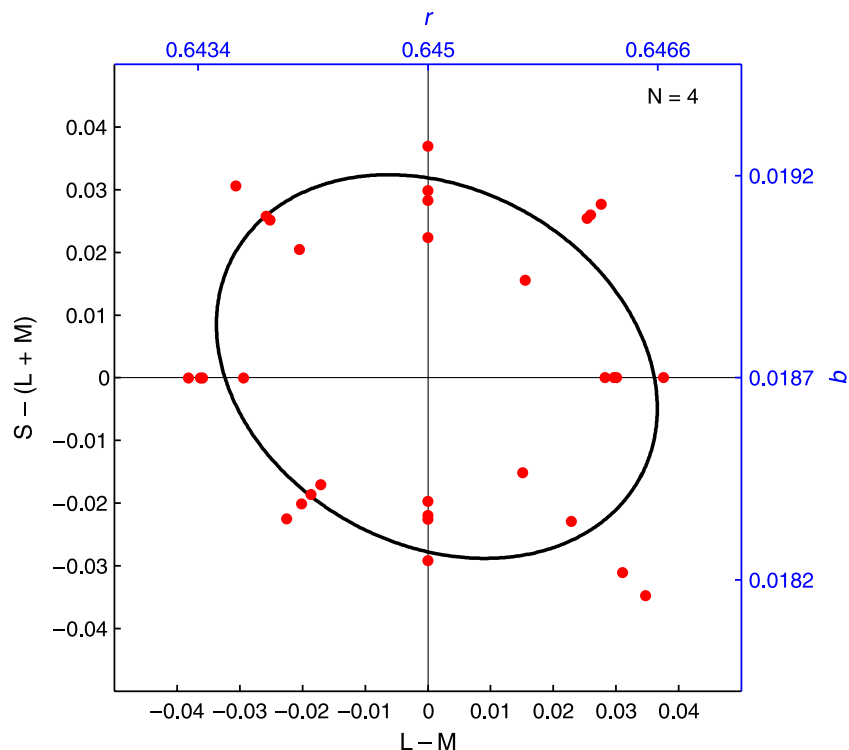


Figure 1. Basic data format and relationship between DKL coordinates and device-independent ( $r, b$ ) coordinates as proposed by MacLeod and Boynton (1979). Sample data show detection thresholds for a uniformly colored disk measured at the adapting white point. Red dots are detection thresholds for four individual observers. The curve is the best fit ellipse to the pooled individual thresholds.

(1979) are depicted in Figure 1, with sample data showing detection thresholds for a uniform disk at the white point, measured for four observers.

## Stimuli

Three types of stimuli were used: uniform colored disks, digital photographs of fruits or vegetables, or synthetic chromatic textures. All stimuli were displayed on top of a uniform background whose color defined the adaptation point.

The main purpose of this study was to investigate chromatic discrimination for natural objects. Three natural stimuli were used (banana, lettuce, and orange), which differ in their chromatic distribution (Figure 2). We also used synthetic chromatic textures to investigate whether any influence of the natural chromatic distribution on

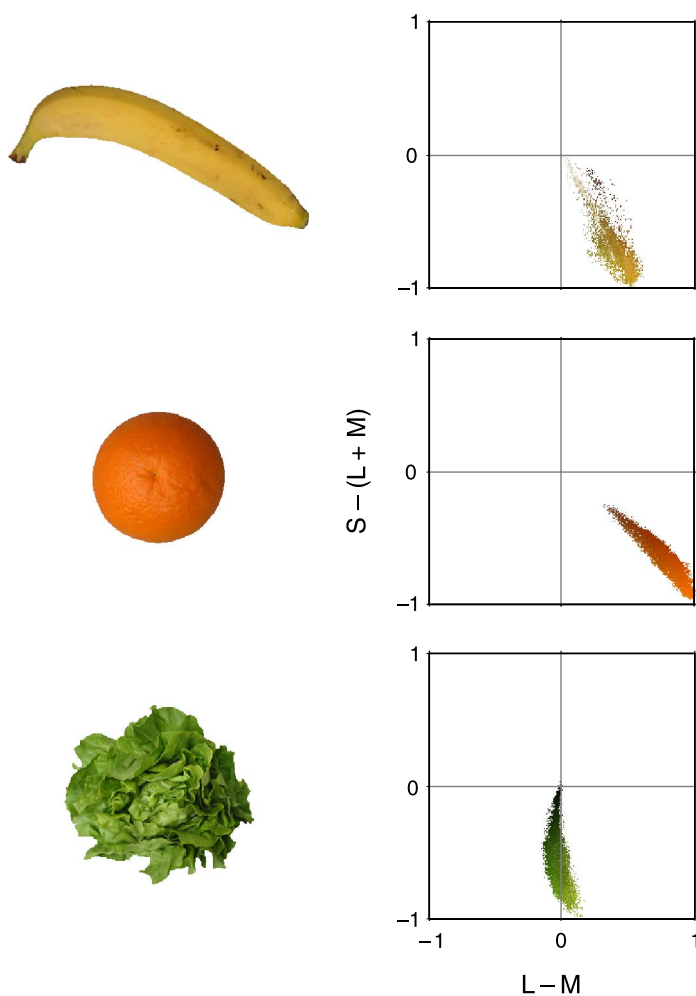


Figure 2. Digital photographs of three natural stimuli and the projection of their chromaticities to the isoluminant plane of DKL color space. The chromaticities mainly vary along a single contrast axis between the most saturated object color and the white point.

discrimination may be due to high-level effects occurring only for the familiar natural objects, or whether such influences can be attributed to low-level spatiochromatic features of the texture instead. For comparison to previous studies, discrimination was always measured for uniformly colored disks subtending  $2^\circ$  visual angle.

The projection of the chromatic distributions of the three natural objects to the isoluminant plane of the DKL color space is shown in Figure 2. The projected chromaticities vary mainly along a single axis between the most saturated color of the object and the white point. In particular, the chromaticities vary either in the lower right quadrant of the isoluminant plane between reddish and greenish-yellow hues (banana, orange) or along the negative part of the  $S - (L + M)$  axis between the white point and yellow-greenish hues (lettuce). One may wonder about the greenish chromaticity of the lettuce varying along the negative part of the  $S - (L + M)$  axis because this axis is often loosely referred to as the “blue-yellow” axis. Confusion occurs because “yellow-blue” is a misnomer, and colors along the  $S - (L + M)$  axis actually vary between purple and yellow-greenish, the color of, for example, lawn and lettuce.

To generate different chromatic distributions for a particular natural object, the whole distribution was rigidly shifted of colors in the isoluminant plane. For illustration, we show images of sample stimuli shifted such that the mean of the chromatic distribution coincides with the white point (Figure 3). The size of the natural stimuli varied between  $8^\circ$  and  $12^\circ$  visual angle.

The synthetic chromatic textures were defined to resemble the natural objects both in chromatic distribution and spatial frequency spectrum. We used two types of synthetic textures to model the spatial frequency characteristic of the natural objects: pink noise, which has an amplitude spectrum of  $1/f$  (slope of  $-1$ ), and brown noise, which has an amplitude spectrum of  $1/f^2$  (slope of  $-2$ ). Pink noise was used because it has been shown that natural images have an average amplitude spectrum of  $-1$  (Field, 1987). Brown noise was used because we found that brown noise more closely resembles the amplitude spectrum of natural textures without object boundaries (details below). As an example for a nonnatural distribution, we used chromatic textures made from uniform noise that has equal energy at all frequency bands. All synthetic textures were squares with a size of  $140 \times 140$  pixels spanning  $5^\circ$  visual angle. The chromatic textures for a particular type of noise were the same across experimental trials. In a control experiment, we used synthetic textures where a new noise texture was generated in each trial. Results of these experiments were qualitatively similar to the results presented here.

To resemble the chromatic distribution of natural objects, we chose the chromatic distribution of the banana as reference for the synthetic textures. Examples of the chromatic textures and their chromatic distributions are shown in Figure 3. The maximum chromatic variation

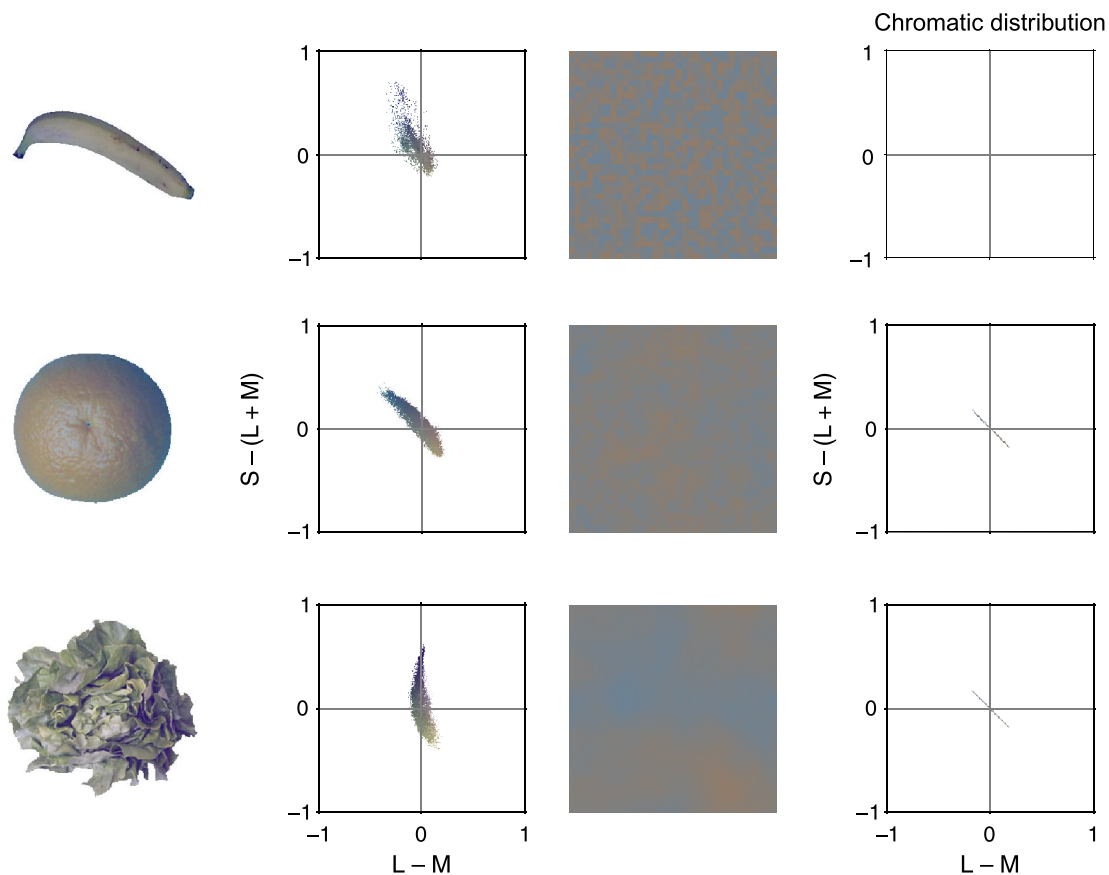


Figure 3. Sample stimuli and the projection of their normalized chromatic distributions to the isoluminant plane of the DKL color space. Both natural stimuli (banana, orange, lettuce, top to bottom, columns 1 and 2) and synthetic textures (uniform, pink, and brown noise, top to bottom, columns 3 and 4) were used in the experiments.

of the banana lies roughly along the second diagonal ( $135\text{--}315^\circ$  azimuth) and has an amplitude of approximately 0.25. The chromaticities of the synthetic textures varied along the line connecting the endpoints of the chromatic distribution with polar coordinates of  $(135^\circ, 0.25)$  and  $(315^\circ, 0.25)$ . In addition, we also tested chromatic textures whose chromaticities varied along the first diagonal ( $45\text{--}225^\circ$  azimuth) and along the cardinal axes of the DKL color space.

The chromatic textures were generated by adjusting the particular noise texture distribution to the desired chromatic distribution. First we generated an achromatic noisy texture with a white noise distribution. For pink and brown noise, this distribution was then Fourier transformed, the amplitude spectrum was reweighted for each frequency to the desired slope, and the result was transformed back to the spatial domain using the inverse Fourier transformation. White noise textures were defined with a larger size of the individual patches ( $4 \times 4$  pixels,  $0.0856^\circ$ ); for the pink and brown noise, the individual patches subtended 1 pixel ( $0.0214^\circ$ ).

The chromatic distribution was defined by the starting and end point of the chromatic distribution in the DKL color space. DKL coordinates of the two points were converted into RGB values, and the difference vector of these values was computed. Computing the difference

vector in RGB space is computationally more efficient because the conversion from DKL to RGB needs not to be done for the whole stimulus but only for two values (start and end point of the chromatic distribution). Finally, the chromatic difference vector was scaled with the achromatic noise texture and the result was added to the starting point of the chromatic distribution.

To model the spatial frequency characteristics of the texture of natural objects, we analyzed their amplitude spectra. It is known that natural images on average have an amplitude spectrum that falls off with a slope of  $-1$  (Field, 1987). Here we were not only interested in the amplitude spectrum of the full image, but also in the amplitude spectrum of a texture without object boundaries. To determine the amplitude spectrum, we first converted the RGB images to the DKL space and decomposed each DKL representation of the images into three two-dimensional images, signaling activation along each of the three cardinal axes of the DKL space, namely,  $L + M$ ,  $L - M$ , and  $S - (L + M)$ . To reduce border effects, we multiplied the images with a Blackman–Harris window function prior to the Fourier transformation. To determine the amplitude spectrum of only the *surface* of the natural objects, without potential contributions of energy at high spatial frequencies from the object edges,

we evaluated the amplitude spectra in a series of overlapping cutouts. Each cutout subtended  $30 \times 30$  pixels and amplitude spectra were evaluated for cutouts at any possible location where the cutout covered only the surface of the object, without inclusion of any object borders. The size of  $30 \times 30$  pixels of the cutout was chosen as the maximum size that could be fitted into all objects. The slope for each of the natural stimuli was determined as the average slope of the amplitude spectra of all cutouts. The mean slope across all stimuli was  $-1.93 \pm 0.20$  SD for all three cardinal axes. This is steeper than a slope around  $-1$  usually found for natural images because we analyzed only the object surfaces without the high-spatial frequency information at the edges. The average slope of the amplitude spectrum of the full images was in the normal range ( $-0.81 \pm 0.17$  SD). We also measured the slope of the amplitude spectrum for the synthetic textures using  $30 \times 30$  cutouts. By definition, the slopes should be 0 for white noise,  $-1$  for pink noise, and  $-2$  for brown noise. The average slopes measured within  $30 \times 30$  cutouts were in the desired range: slopes were for white noise  $0.04 \pm 0.14$  SD, for pink noise  $-1.04 \pm 0.15$  SD, and for brown noise  $-2.32 \pm 0.16$  SD.

## Subjects

Four observers (C.H., D.P., M.G., and M.O.) participated in the experiments. All observers except one of the authors (M.G.) were naive as to the purpose of the experiment. All observers were experienced psychophysical observers who had participated in previous experiments.

## Procedure

The procedure was similar to the one employed by Krauskopf and Gegenfurtner (1992). Observers were seated in front of the monitor at a distance of 0.60 m in a dimly lit room and instructed to fixate the center of the screen, which was uniformly colored. In each experimental trial, four stimuli were presented for 500 ms in a  $2 \times 2$  arrangement. The bounding box of each stimulus had a constant distance of  $1^\circ$  visual angle from the center of the screen. Three of the presented stimuli were identical (test stimuli) whereas the fourth one (comparison stimulus) differed slightly in chromaticity. The position of the comparison stimulus in the  $2 \times 2$  arrangement was randomly varied in each trial. The observer's task was to indicate the position of the comparison stimulus (odd one out) by pressing the appropriate one of four buttons. Feedback was given after each response. For each test color, discrimination thresholds were measured in eight different comparison directions ( $0^\circ$ ,  $45^\circ$ ,  $90^\circ$ ,  $135^\circ$ ,  $180^\circ$ ,  $225^\circ$ ,  $270^\circ$ , and  $315^\circ$ ) relative to the mean chromaticity of the test stimulus. Test and comparison chromaticities were specified in the isoluminant plane of the DKL color space.

The chromaticities of the comparison stimulus were varied by a rigid shift of the whole chromatic distribution in the isoluminant plane in the comparison direction. This transformation shifts the mean of the distribution to the comparison color but keeps the position of the chromaticities relative to the mean chromaticity constant. The amount or amplitude of this shift necessary for a correct discrimination at 79% of the trials was determined using an adaptive double-random staircase procedure. After three consecutive correct responses, the comparison amplitude was decreased; after an incorrect response, it was increased. In each session, one up- and one down-staircase for each of the eight comparison directions were randomly interleaved. Each staircase terminated after four reversals.

Discrimination thresholds were measured under two different conditions of adaptation, as defined by the chromaticity of the background. In the first condition, chromatic discrimination was measured at the adaptation point; in the second condition, discrimination was measured at test locations away from the adaptation point.

In the first condition, discrimination was investigated at the location in color space to which the observer was adapted; that is, the test color was the same as the background color (test amplitude of zero) and the comparison stimuli were excursions from the chromaticity of the background. For the homogeneously colored disk, this condition corresponds to a detection task. For the natural stimuli and the chromatic textures, the mean chromaticity of the stimuli was the same as the chromaticity of the background. Discrimination at nine different adaptation points was investigated by changing the background color. The adapting background color was either the white point or one out of eight equally spaced colors in the isoluminant plane. These eight colors all had the same amplitude of 0.5, but different chromatic directions of  $0^\circ$ ,  $45^\circ$ ,  $90^\circ$ ,  $135^\circ$ ,  $180^\circ$ ,  $225^\circ$ ,  $270^\circ$ , or  $315^\circ$ . In this condition, the mean chromaticity of the test stimulus coincided with the chromaticity of the adaptation point.

In the second regime, the background was always gray; that is, the adaptation point was fixed at the white point and the test stimuli were excursions from this point in eight test directions ( $0^\circ$ ,  $45^\circ$ ,  $90^\circ$ ,  $135^\circ$ ,  $180^\circ$ ,  $225^\circ$ ,  $270^\circ$ ,  $315^\circ$ ) with a test amplitude of 0.5. In this condition, the mean chromaticity of all stimuli differed from the chromaticity of the adaptation point.

## Data analysis

To determine thresholds, we pooled the observers' responses for the up- and the down-staircase for each comparison direction. Psychometric functions were fitted to the individual observer's data using the `psignifit` toolbox for Matlab (Wichmann & Hill, 2001) to derive 79% difference thresholds for each of the eight comparison directions. To summarize the data, we fitted ellipses to the eight thresholds using a direct least squares

procedure (Halíř & Flusser, 1998). As in previous studies (Poirson, Wandell, Varner, & Brainard, 1990), we found that the ellipses describe the data well. To account for small asymmetries, we allowed the centers of the ellipses to vary. To obtain ellipses for data averaged across observers, we fitted ellipses to the pooled thresholds of all observers, as suggested by some authors as being the most robust method (Wyszecki & Fielder, 1971a; Wyszecki & Stiles, 1982; Xu, Yaguchi, & Shioiri, 2002). Alternatively, we fitted ellipses to the thresholds averaged across observers. As a third alternative, we also fitted ellipses to the thresholds of the individual observers and then averaged across the parameters of ellipses. All of these methods provided similar results.

To determine the reliability of the orientation of the discrimination ellipses, we employed a bootstrap procedure similar to the method described by Alder (1981). For each threshold measured in the eight comparison directions, 1,000 simulated thresholds were drawn from normal distributions centered at the measured thresholds. The standard deviation of these distributions was estimated

from the bootstrap confidence intervals of each threshold provided by the psignifit toolbox for Matlab (Wichmann & Hill, 2001). Ellipses were then fitted to the simulated thresholds and the 95% confidence interval for the orientation of the major axis was computed.

## Results

The results are organized in two sections. In the first section, we present results for discrimination at the adaptation point; and in the second section, we present results for discrimination away from the adaptation point.

### Discrimination at the adaptation point

Figure 4 shows the discrimination ellipses measured at the adaptation point defined by the gray background on

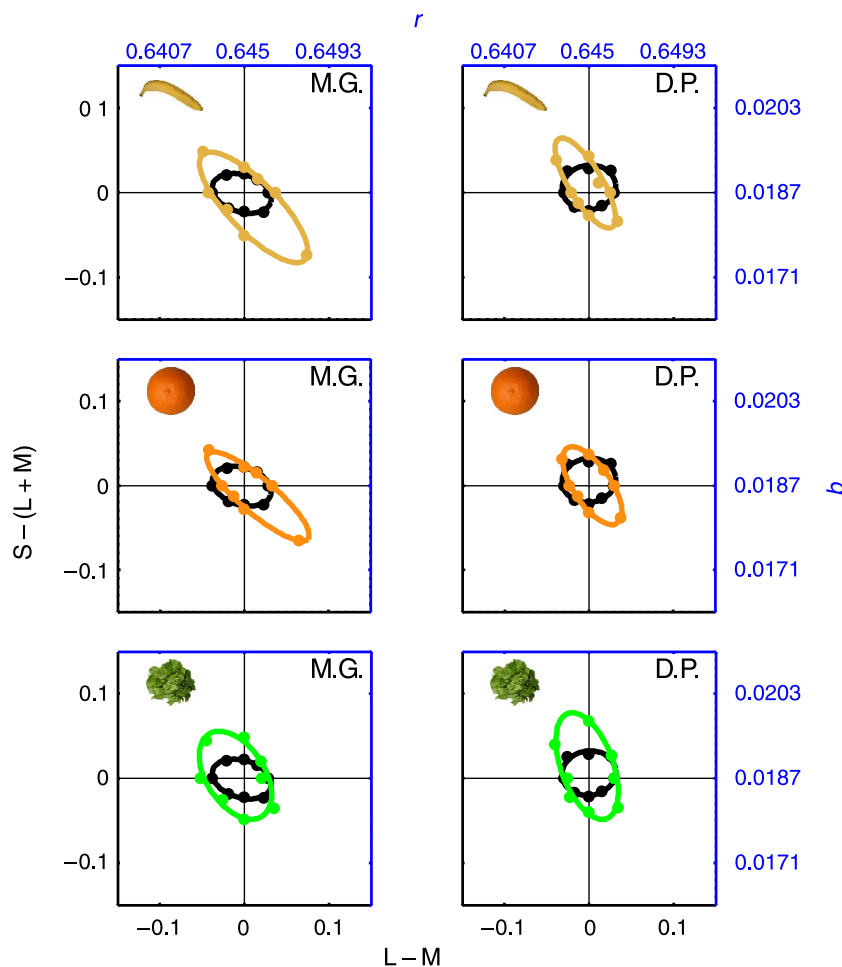


Figure 4. Discrimination ellipses for natural stimuli and uniform disks at the adaptation point. Discrimination ellipses for the natural stimuli (banana, orange, and lettuce, top to bottom) are elongated in the direction of maximal chromatic variation compared with the almost circular discrimination ellipses for the uniform disks (black). Data points are discrimination thresholds for the two observers (M.G. and D.P.). The curve is the best fit ellipse to the thresholds.

which the stimuli were presented. Discrimination ellipses for two observers are shown for natural stimuli (banana, orange, and lettuce) and are compared with discrimination ellipses obtained for a uniformly colored disk.

The discrimination ellipses for all natural stimuli show a distinct elongation different from the almost circular ellipses obtained for the uniform disks. For example, the ellipse for the banana shows a clear elongation along the second diagonal, which is the same direction along which the chromaticities of the banana vary most (Figure 3). Overall, the direction of the major axis of the ellipses for the natural stimuli seems to follow the direction of maximal chromatic variation. This means that shifts of the chromatic distribution in directions where there was already considerable chromatic variation in the stimulus were harder to detect than shifts in those directions where there was little variation in the stimulus. In contrast, thresholds for comparison directions away from the direction of maximal variation were similar to those for the uniformly colored disk.

Next we measured chromatic discrimination at the adaptation point with synthetic textures. The objective of using synthetic textures was twofold. First we wanted to isolate characteristic features of the natural stimuli to clarify whether the differences in threshold contours might be attributed to higher or lower level visual effects. Second, we wanted to investigate whether the observed elongation always follows the direction of maximal variation in the stimulus. This can be tested with synthetic textures whose chromatic distribution can be rotated to arbitrary angles.

In the first set of experiments, we used synthetic textures with spatial frequency distributions that resemble the distributions found in natural objects (pink and brown noise) as well as a distribution with a flat amplitude spectrum (white noise). All synthetic chromatic textures had the same chromatic distribution, oriented along the second diagonal. We compared discrimination thresholds for the three types of synthetic textures with the discrimination thresholds of the banana (Figure 5).

The discrimination ellipses for all synthetic textures were elongated along the direction of maximal chromatic variation, similar to the ellipses for the banana (Figure 5). This clearly shows that the observed effect can be obtained with synthetic textures. The higher discrimination thresholds along the direction of maximal chromatic variation are not influenced by higher level knowledge or the familiarity of the natural objects.

So far we have only used stimuli with chromatic distributions that vary along the second diagonal, between bluish and orange hues. In the next series of experiments, we rotated the chromatic distribution in different directions. This allows us to investigate whether the elongation of the discrimination ellipses was indeed caused by the direction of the maximal variation in the chromatic distribution. Brown noise stimuli whose chromatic distribution varied along four different directions were tested.

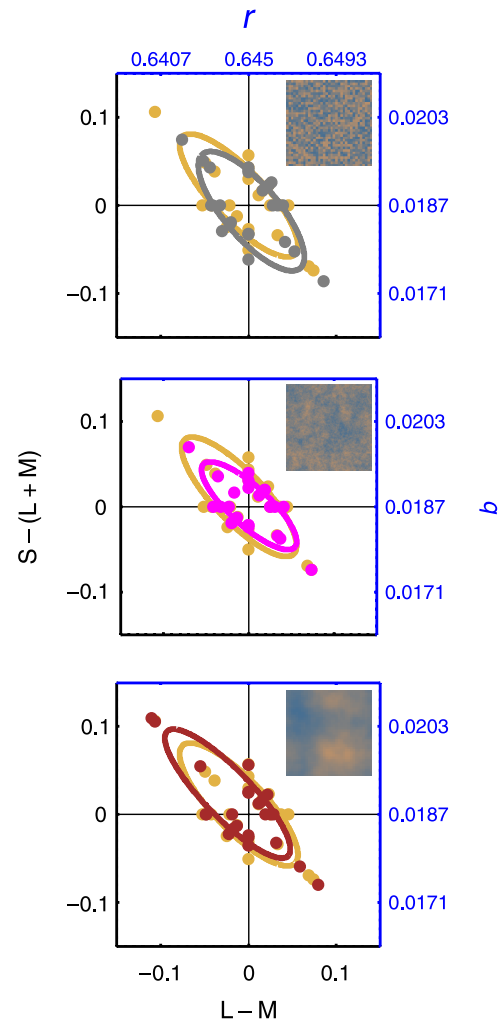


Figure 5. Discrimination ellipses for the synthetic textures compared with those for the banana (yellow). The synthetic textures were of similar chromatic variation as the banana but differed in spatial distribution: white noise (gray), pink noise (pink), and brown noise (brown). Discrimination contours for all synthetic textures were similar to those for the banana. Data points are discrimination thresholds for three individual observers (C.H., M.G., and M.O.). The curve is the best fit ellipse to the pooled individual thresholds. The insets depict examples of the synthetic textures whose contrast has been enhanced for better visibility.

The distribution varied either along the cardinal directions or along intermediate directions (Figure 6). In all cases, the direction of the elongation of the ellipses closely follows the direction of the chromatic distribution.

Besides discrimination at the gray adaptation point, we also measured discrimination at eight different adaptation points. Discrimination was measured for the uniformly colored disk, the banana, and the brown noise texture (Figure 7). Ellipses in the center of Figure 7 show the threshold contours for discrimination at the gray adaptation point. The mean chromaticity of the test stimuli was gray and the chromaticity of the comparison stimulus

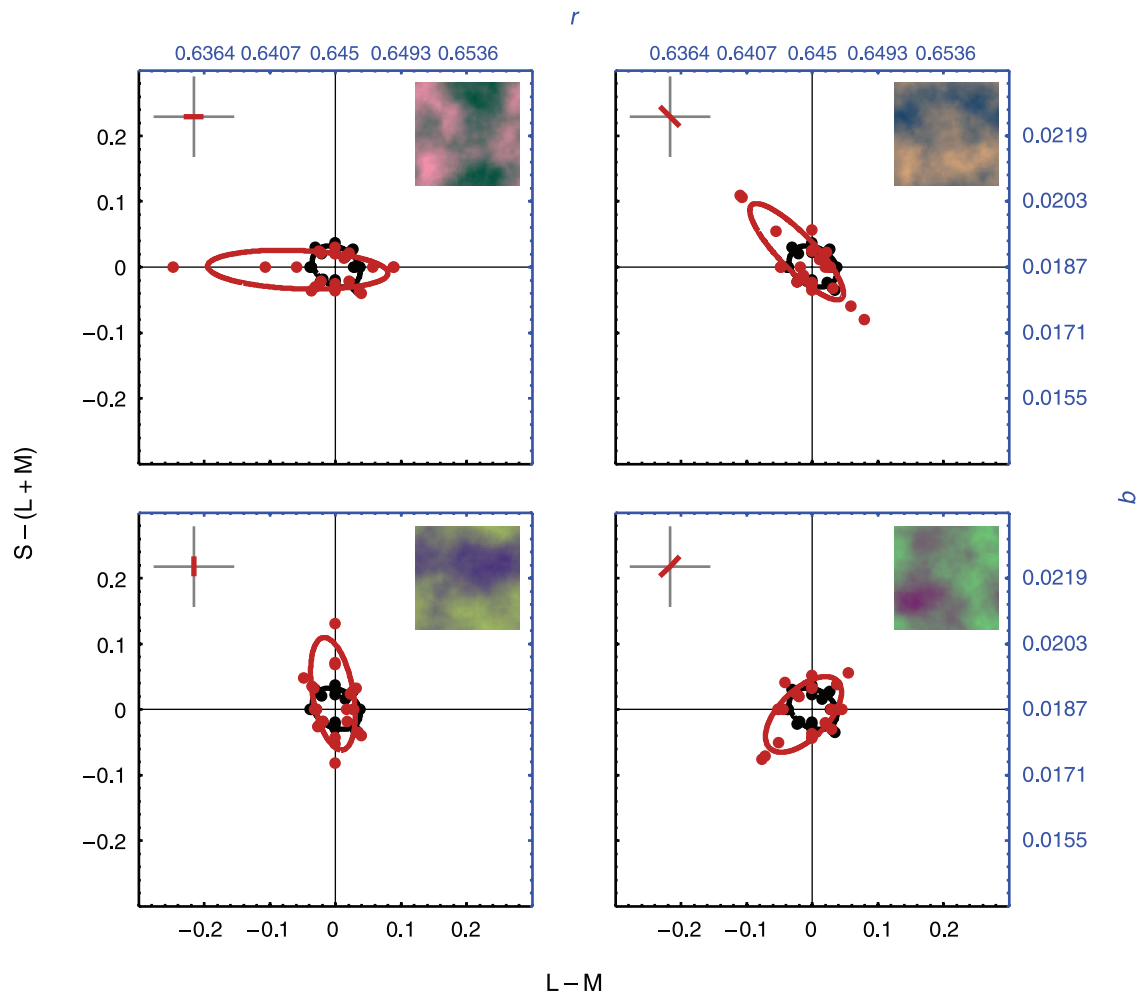


Figure 6. Discrimination ellipses for brown noise stimuli are elongated in the direction of maximal chromatic variation. Chromatic directions of  $0^\circ$  (top left),  $135^\circ$  (top right),  $90^\circ$  (bottom left), and  $45^\circ$  (bottom right) were tested, depicted by the top left inset. Data points are discrimination thresholds for three individual observers (C.H., M.G., and M.O.). Format is identical to the previous figure.

was an excursion from the adaptation point in one of eight comparison directions. For the eight different adaptation points, the mean chromaticities of the test stimuli were identical to the location indicated by the crosses in Figure 7. We found at most adaptation points a pattern of results similar to the results at the gray adaptation point: Discrimination ellipses for the banana and for a brown noise chromatic texture were larger and elongated compared to the ellipses obtained for a uniformly colored disk.

To further quantify the data, we determined the area and the eccentricity of each discrimination ellipse. We plotted the area and the eccentricity of the ellipses, averaged across subjects, for each of the nine adaptation points. Discriminability, quantified as the area of the discrimination ellipse, was almost constant for all adaptation points and all stimuli (Figure 8A). In contrast to the almost identical area for all stimuli, the eccentricities differed considerably for the different stimuli (Figure 8B): For all but one adaptation point ( $225^\circ$ ), the eccentricity of

the discrimination ellipses for the banana and the brown noise texture was higher than for the uniform disks. This shows that discrimination at the adaptation point is different for chromatic textures compared to uniform disks, largely independent of the adapting color.

Figures 7 and 8A show that not only the chromatic textures had elongated discrimination ellipses of rather high eccentricity, but that elongated ellipses also occur for the uniform disk, in particular at one adaptation point ( $225^\circ$ ). To further analyze whether only the ellipses for the chromatic textures show a distinctive elongation in the direction of the chromatic distribution, we plot in Figure 9 eccentricity versus orientation of the ellipses. Data are shown for the individual observers' ellipses for the adaptation points presented in Figure 7.

The orientations of the major axis of the ellipses for the banana and the brown noise stimuli clustered between  $120^\circ$  and  $135^\circ$  azimuth close to the direction of maximal variation of the chromatic distribution. The orientations for the chromatic textures were better defined than those

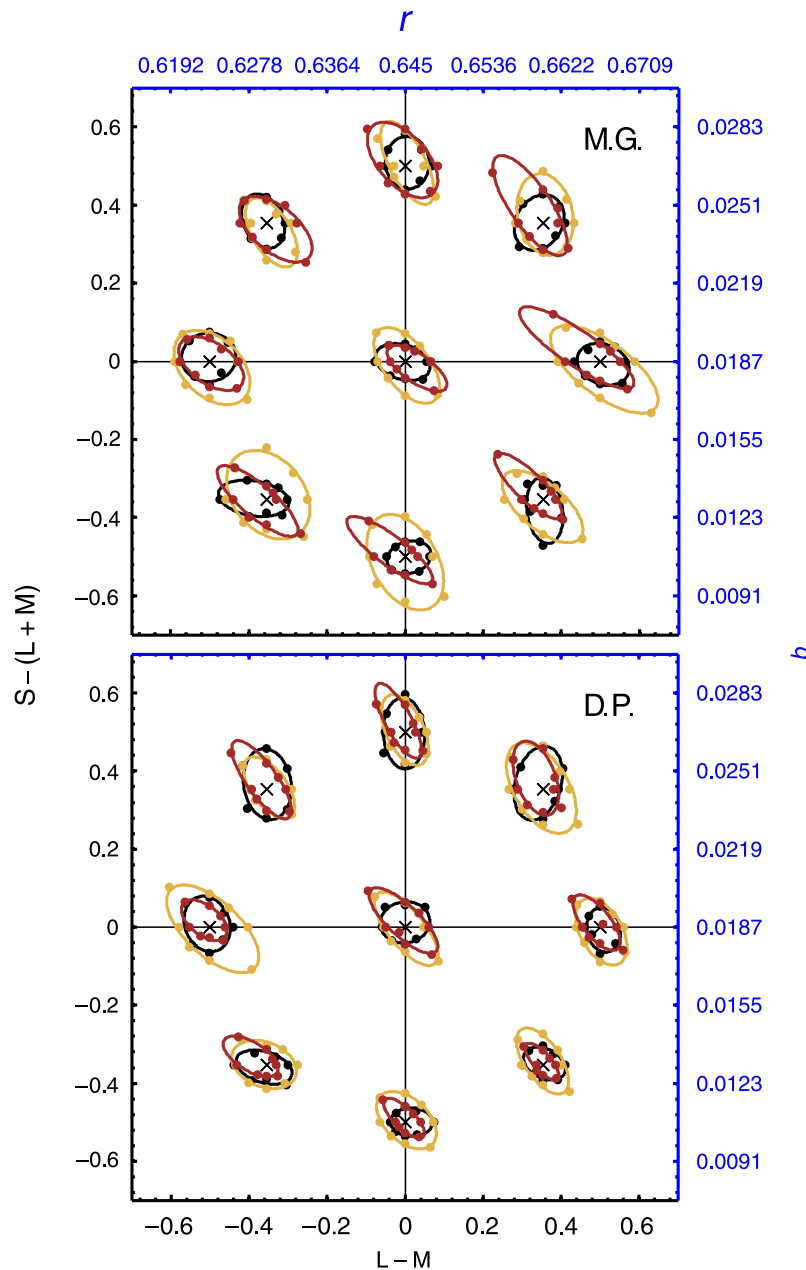


Figure 7. Discrimination at nine different adaptation points (crosses). In most cases, discrimination ellipses for the banana (yellow) and for a brown noise chromatic texture (brown) are larger and elongated compared to the ellipses obtained for a uniformly colored disk (black). Data are shown for two observers (M.G. and D.P.). The ellipses have been magnified by a factor of two.

for the uniform disk. Applying a bootstrap procedure showed that the medians of the confidence intervals for the orientations of the discrimination ellipses for the banana and the brown noise texture were smaller (subject M.G.:  $\pm 45^\circ$ , brown noise,  $\pm 27^\circ$ , banana; subject D.P.  $\pm 29^\circ$ , brown noise,  $\pm 31^\circ$ , banana), compared with the median of confidence intervals for the uniform disk (subject M.G.:  $\pm 84^\circ$ ; subject D.P.:  $\pm 77^\circ$ ). The orientations of the ellipses for the uniform disk are almost equally distributed and show no preference for any orientation. Overall, the small elongations of the discrimination ellipses for the uniform disk did not follow a particular

pattern and were not caused by the chromatic distribution of the stimuli, whereas the orientations of the ellipses for the banana and the brown noise stimulus were consistently close to the direction of maximal chromatic variation.

Overall, we find that discrimination ellipses for natural stimuli and synthetic chromatic textures with a distribution of chromaticities differ from those for uniform disks. Whereas discrimination ellipses for uniform disks were largely circular, those for chromatic textures were elongated in the direction of the maximum chromatic variation of the stimuli.

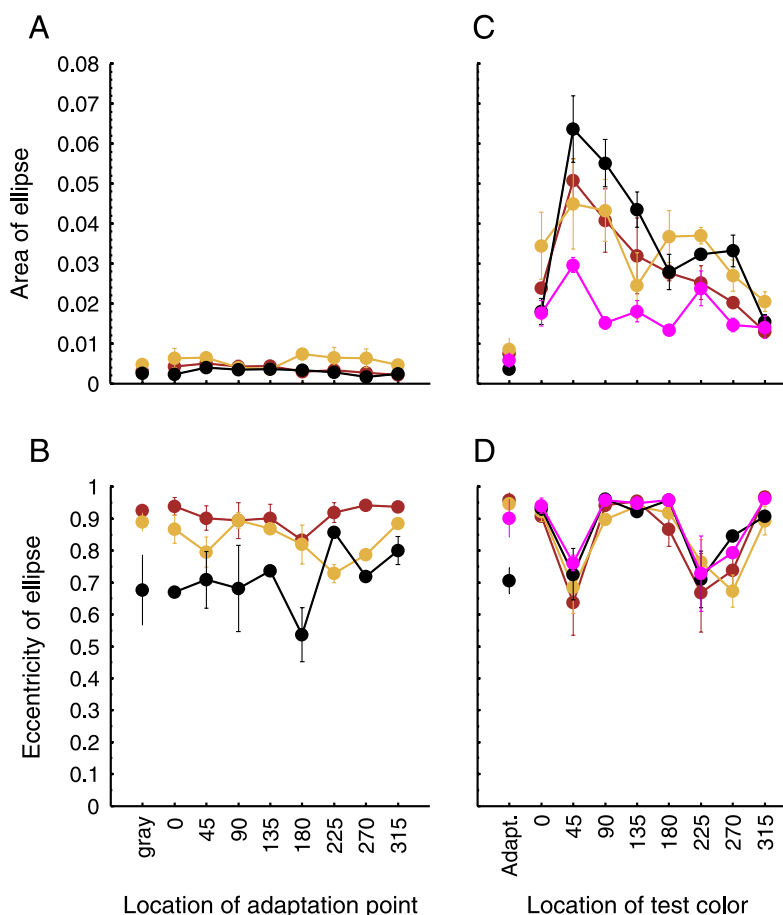


Figure 8. Area and eccentricity of the ellipses at the adaptation point (A, B) and away from the adaptation point (C, D). Ellipse parameters are determined from ellipses fitted to the pooled data of two (A, B) or three (C, D) observers. Colors denote the different stimuli: uniform disk (black), banana image (yellow), pink noise texture (pink), and brown noise texture (brown). (A, B) Ellipse parameters for nine different adaptation points are based on the data presented in Figure 7. (C, D) Ellipse parameters away from the adaptation point are based on the data presented in Figure 10.

### Discrimination away from the adaptation point

In the second set of experiments, we investigated discrimination away from the adaptation point. In these experiments, the subjects remained adapted to the white point. The chromatic distribution of the stimuli was shifted in such a way that the mean chromaticity of the stimuli was the same as the chromaticity at the test location. Figure 10 shows the discrimination ellipses for the uniformly colored disk, banana, pink, and brown noise at eight test locations away from the adaptation point, fitted to the thresholds of three observers. For comparison, we also show the discrimination ellipses at the adaptation point already presented in Figures 4 and 5.

The discrimination thresholds for all stimuli were lowest when they were presented at the adaptation point. We found that at test locations away from the adaptation point, thresholds for all stimuli were similar and elevated compared with the discrimination thresholds at the adaptation point. Threshold contours for the banana, the

textures, and the uniform disk at these test locations were almost identical and exhibited an elongation along the contrast axis connecting the white point and the color at the test location instead of the elongation in the direction of the chromatic distribution found at the adaptation point.

The difference in the elongation and the elevation of the ellipses for the different stimuli becomes more obvious in Figure 8C, where the area of the ellipses is plotted across the test locations. The area is smallest at the adaptation point and increases at test locations away from the adaptation point, notably in the upper two quadrants. In Figure 8D, the eccentricity of the ellipses is plotted for all test locations. Whereas the ellipses for the uniform disk and the textured stimuli differ markedly in their eccentricity at the adaptation point, there are no such differences at test location away from the adaptation point. The discrimination ellipses at the test locations  $45^\circ$  and  $225^\circ$  azimuth are more circular. This is in agreement with results reported by Krauskopf and Gegenfurtner (1992). As Krauskopf and Gegenfurtner pointed out, these results indicate that discrimination is not mediated solely by

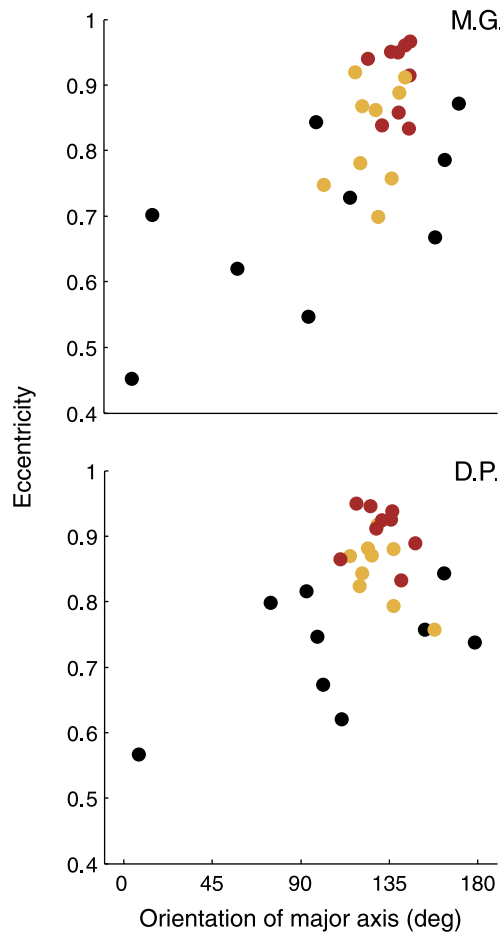


Figure 9. Eccentricity of ellipses plotted against the orientation of the major axis for the data presented in Figure 7. The orientations of the ellipses for the banana (yellow) and the chromatic brown noise texture (brown) are close to the orientation of the chromatic variation ( $135^\circ$ ). On the other hand, the orientations of the ellipses for the disk (black) are more widely spread. The well-defined angles of the ellipses for stimuli with a chromatic variation are also reflected in the median 95% bootstrap confidence intervals. The medians of the confidence intervals across the nine adaptation points were smaller for the stimuli with a chromatic variation (subject M.G.:  $\pm 45^\circ$ , brown noise,  $\pm 27^\circ$ , banana; subject D.P.  $\pm 29^\circ$ , brown noise,  $\pm 31^\circ$ , banana), compared with the median of confidence intervals for the uniform disk (subject M.G.:  $\pm 84^\circ$ ; subject D.P.:  $\pm 77^\circ$ ).

mechanisms tuned to the cardinal axes of color space because a cardinal model would predict that all discrimination ellipses are oriented along the cardinal axes ( $0^\circ$  or  $90^\circ$ ) and consequently cannot account for the measured oblique orientation at test locations displaced along intermediate axes (chromatic direction  $45^\circ$ ,  $135^\circ$ ,  $225^\circ$ , and  $315^\circ$ ).

Overall, discrimination ellipses for stimuli away from the adaptation point were larger than those at the adaptation point. Further, in most cases, ellipses were elongated along the contrast axis connecting the white

point and the chromaticity at the test location. This increase in thresholds is in accordance with Weber's law. Interestingly, there is no additional increase in thresholds due to the variability within the textured stimuli. Presumably, the effect of this variability is small compared to the increase in threshold due to the difference between adaptation and test color. This issue has to be addressed in future experiments.

## Discussion

### Summary of findings

We have investigated chromatic discrimination for natural objects. Resulting discrimination thresholds were compared with thresholds for uniformly colored disks and synthetic chromatic textures. We found that at the adaptation point chromatic discrimination for natural objects with a distribution of chromaticities differed from discrimination for uniform disks. This chromatic distribution affects the threshold magnitude and changes the shape of the discrimination ellipses: Whereas discrimination ellipses for uniform disks were largely circular, the discrimination ellipses for natural objects were elongated in the direction of maximum variation of the chromatic distribution of the stimuli.

A similar selective elongation of the discrimination ellipses was found for synthetic chromatic textures. We found the effect to be similar for textures with different amplitude spectra (white, pink, and brown noise), showing that the slope of the amplitude spectrum over the tested range ( $0$ ,  $-1$ ,  $-2$ ) is not a critical parameter for chromatic discrimination. Further, the similarity between discrimination for natural objects and for synthetic stimuli showed that the differences in discrimination contours were not caused by high-level vision effects, such as color memory, arising due to the familiarity of the natural stimuli. Rather, it indicates that the differences in threshold contours can be attributed to low-level stimulus features. It has been shown that the memory color of familiar objects modulates their appearance (Hansen et al., 2006). For chromatic discrimination, we found no high-level influence of familiar natural objects. Instead, our results showed that chromatic discrimination can be influenced by the chromatic distribution of the stimuli: For both natural objects and synthetic textures, thresholds increased along the direction of maximal chromatic variation of the chromatic distribution.

These effects were confined to discrimination at the adaptation point. No such differences between the different types of stimuli were found for discrimination away from the adaptation point. Away from the adaptation point, thresholds for all stimuli were elevated compared with those at the adaptation point. In other words, chromatic

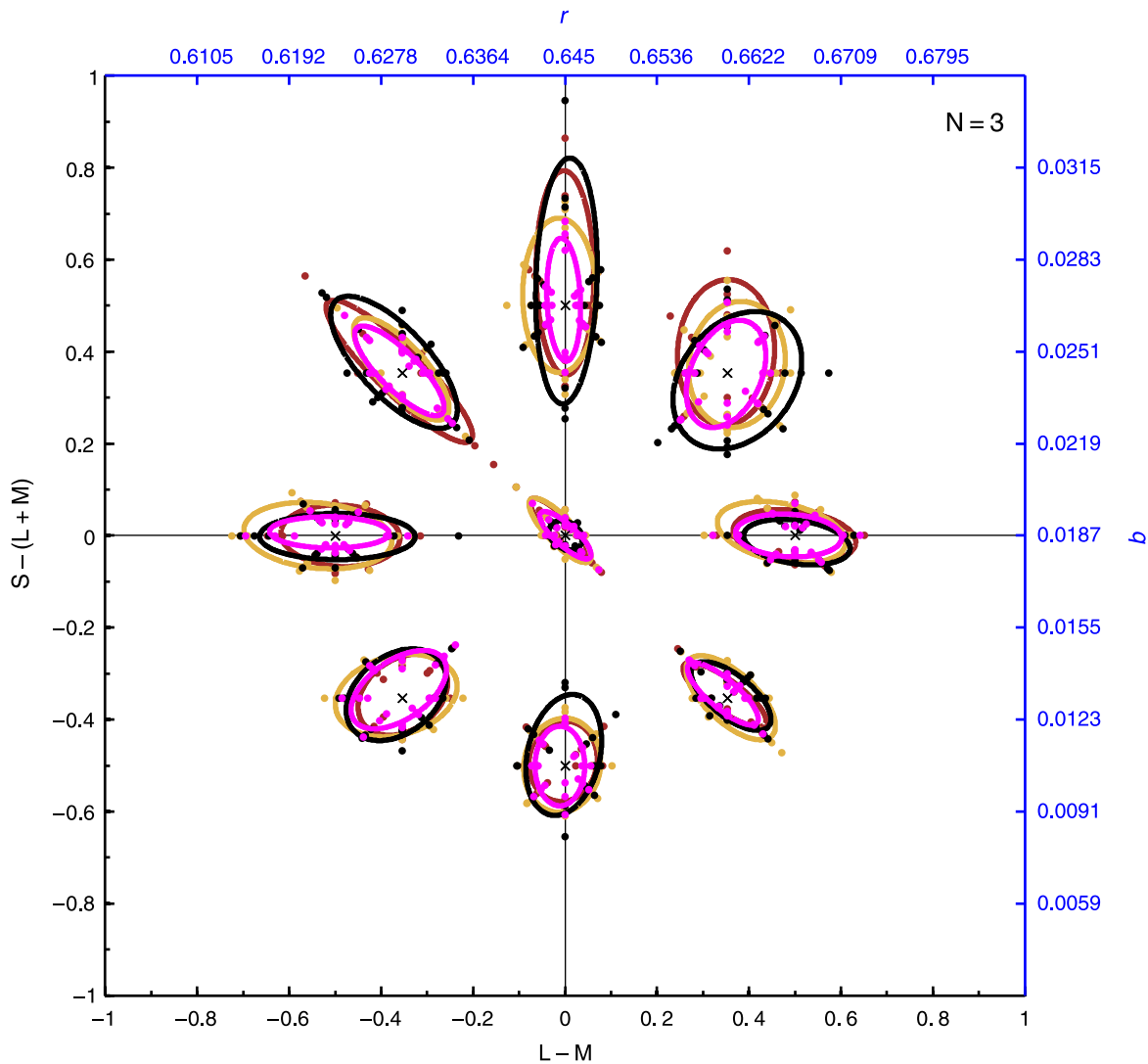


Figure 10. Discrimination away from the adaptation point. Ellipses for a uniformly colored disk (black), a digitized banana image (yellow), and a pink (pink) and brown (brown) noise textures at the gray adaptation point and at eight test locations away from the adaptation point. The crosses indicate the chromaticity at the test location. Data points are discrimination thresholds for three individual observers (C.H., M.G., and M.O.). The curve is the best fit ellipse to the pooled individual thresholds.

discrimination is best at the adaptation points, in agreement with earlier studies (Krauskopf & Gegenfurtner, 1992). Highest thresholds were measured at the test location with  $45^\circ$  azimuth (Figure 10). In general, thresholds in the upper two quadrants were elevated compared with thresholds in the lower two quadrants, indicating that color vision is less sensitive at discriminating bluish hues and hues along the purple line.

Discrimination ellipses for stimuli with a chromatic distribution were determined by the amplitude and the direction of both the chromatic distribution and the shift away from the adaptation point. An increase of the distance between the adaptation point and the test location elevated discrimination thresholds. Depending on the amplitude of the shift, this threshold elevation was so big that it masked the effect of the chromatic distribution. Another reason that we have not found any effect of the

chromatic distribution away from the adaptation point might be due to the particular choice of the chromatic texture, as discussed in the following.

### No effect of the chromatic distribution away from the adaptation point?

For chromatic discrimination away from the adaptation point, we found no effect of the chromatic texture, which might be partly caused by the particular *orientation* of the chromatic distributions we employed. In our experiments, the variation of the chromatic distribution was along the second diagonal, from  $135^\circ$  to  $315^\circ$ . For shifts of the test color in these directions, ellipses for homogeneous disks already had the largest variation along this axis, and the additional chromatic variation of the stimulus may

consequently be masked. On the other hand, one may expect effects for shifts of the test color orthogonal to the chromatic distribution of the stimulus, that is, along the main diagonal. However, discrimination ellipses for homogeneous disks were already relatively large and rounded away from the adaptation point along these directions ( $45^\circ$  and  $225^\circ$ ). Following this argument, effects away from the adaptation point should occur for chromatic distributions varying along the first diagonal at test locations shifted along the second diagonal. In a pilot study, we have found evidence for effects away from the adaptation point.

Given that the main purpose of our study was to determine discrimination thresholds for natural stimuli, and given that these stimuli were rather limited in their chromatic variation, we cannot draw any firm conclusions about the interaction of the chromatic variation within each test object with the variation due to changes in adaptation. Therefore, in future studies using synthetic textures, we plan to investigate the interaction between orientation and amplitude of the chromatic distribution and the test locations in more detail.

## Comparison to previous work

Traditionally, chromatic discrimination has been studied with uniform, homogeneous colors (Brown & MacAdam, 1949; MacAdam, 1942), and only a single previous study has investigated chromatic discrimination of stimuli having a chromatic distribution (te Pas & Koenderink, 2004). In their study, te Pas and Koenderink (2004) investigated discrimination for different chromatic distributions that were specified in RGB space. Observers had to report the orientation of two half-fields of different textures, which could be oriented either horizontally or vertically. They found higher discrimination thresholds for textured stimuli than for uniform stimuli. Thresholds differed for different test colors of the stimuli, but these differences were attributed to variations in luminance between the stimuli. In general, the results of te Pas and Koenderink are difficult to compare to our findings because the stimuli were specified in RGB space, which confounds luminance and pure chromatic variation. Further, thresholds were measured only in one direction, and the chromatic distribution was not only rigidly shifted in color space, as in this study. Instead, the extent of the chromatic distribution was changed during the threshold measurement. It was either broadened to white (i.e., in a direction of the highest luminance of the monitor primaries), to model changes due to specular reflectance, or rotated, to model changes in material.

A more indirect effect of the chromatic distribution on discrimination was investigated by Zaidi et al. (1998). Observers adapted either to a uniform background or to a variegated background made of randomly arranged squares having one of two colors along the cardinal

L – M axis. After the adaptation interval, chromatic discrimination was measured. The screen was divided either vertically or horizontally, resulting in homogeneously colored halves that differed in chromaticities. The chromaticities were picked from the endpoints of various intervals on the L – M axis that differed in length but were centered at a fixed point. When the observers were adapted to a textured background, thresholds were higher than when they were adapted to a uniform background. Thresholds for the textured background were highest when the test color was the same as the spatial average of the background textures and decreased when the test color moved away from the average. For uniform adapting fields, discrimination was best at the adaptation point and increased with increasing distance of the test chromaticity from the adaptation point. In our study, we used a homogeneous background and measured discrimination for chromatic textures. We find that discrimination at the adaptation point was determined by the amplitude and the direction of the chromatic variation.

Various authors have studied the segmentation of chromatic textures (D’Zmura & Knoblauch, 1998; Gegenfurtner & Kiper, 1992; Goda & Fujii, 2001; Hansen & Gegenfurtner, 2006; Li & Lennie, 1997; Webster & Mollon, 1991, 1994). In these studies, textured targets were embedded in a textured background and not spatially separated by a homogeneous background, as in this study. Also, previous studies differ in their schemes used to modulate the target texture compared to the background texture. Despite these differences, all studies found that thresholds are elevated considerably when background and target distributions were modulated along similar directions in color space. In agreement with these findings, we have found the largest threshold elevations when the chromatic distribution was shifted along the axis of maximal variation of the chromaticities in the stimulus, such that the chromaticities of the test and the comparison stimuli mostly varied along the same direction. Because of the different stimuli that vary both in layout and definition of the chromatic distributions, other aspects are difficult to compare across studies.

## Models and mechanisms for chromatic texture discrimination

Unfortunately, none of the elaborate models that are available for spatial vision extends to the color domain. Typical “back-pocket-models” for spatial pattern sensitivity contain three main stages (Bergen & Adelson, 1988; Bergen & Landy, 1991; Watson & Ahumada, 1989; Wilson & Reagan, 1984): At the first stage, the image is convolved with a set of filters that differ in orientation and scale. At the second stage, these filters undergo a static nonlinearity. Finally, noise may be added to the nonlinearly transformed response of the filter bank, and responses are fed into a final decision stage. Such models

are based on a wide variety of experimental data that have been replicated in many different laboratories under standardized conditions (Carney et al., 1999, 2000; Chen & Tyler, 2000; Klein, 1993; Watson, 2000; Watson & Ahumada, 2005; Watson & Ramirez, 1999). These models predict performance in simple luminance detection and discrimination experiments, as well as for complex texture patterns.

In the color domain, discrimination data have been frequently obtained under highly different conditions, and the results are presented in many different color spaces. Although it is possible, in principle, to convert between different color spaces, there are other aspects such as the sampling of the stimuli that make it difficult to compare such data.

Existing models of chromatic difference prediction often transform the image into an opponent color space with three channels (black–white, red–green, yellow–blue), sometimes in multiple spatial frequencies and orientations, and then compute the point-by-point difference between a test and a reference image for two-dimensional planes in all channels. In the next step, these difference planes may be combined to a single two-dimensional difference image or a single difference number (Daly, 1993; Lovell, Párraga, Troscianko, Ripamonti, & Tolhurst, 2006; Zhang & Wandell, 1996, 1998). The common feature of these models is the stage where a local, point-by-point difference is computed. For example, the spatial extension of CIE Lab into S-CIELAB (Zhang & Wandell, 1996, 1998) uses a spatial blurring of three color-opponent planes and then computes the pixel wise difference between images. Another class of models starts with a number of global image descriptions, such as color histograms or Fourier spectra. Image differences are then determined based on the difference in these global descriptors. Models of this type are frequently used in the domain of content-based image retrieval to determine differences between images (e.g., Neumann & Gegenfurtner, 2006). These models were designed to globally evaluate suprathreshold differences and may not be ideally suited for evaluating threshold-level differences between small textured patches. A particular subclass of global models may be better suited, which have been proposed to predict detection and discrimination thresholds for patterns that vary in color or luminance (Chen, Foley, & Brainard, 2000; Goda & Fuji, 2001; Hansen & Gegenfurtner, 2006). These models first compute the global response of a set of chromatic detection mechanisms to the image chromaticities. Mechanism responses are computed for two images, and the response difference is used as a measure of discriminability. Whereas global models leave out the spatial aspects of the stimuli, local models take the spatial and chromatic aspects into account, but not the second-order color statistics of the chromatic distributions of the stimuli.

As outlined above, for chromatic texture discrimination, one may distinguish between two different types of

conceptual models, which are based on either local or global processing. Local models imply that thresholds are determined by local information and not from the chromatic distribution. Global models, on the other hand, assume that observers cannot precisely match the spatial locations between any two images, and that the global chromatic distribution determines discriminability. Global models are in accordance with findings that chromatic discrimination across eye movements is poor (Sachtler & Zaidi, 1992). In the following, we argue that global models of chromatic texture discrimination are better suited to account for the effect of the chromatic distribution on discrimination as studied in the present article.

In local models, discrimination thresholds are determined from the local comparison of matched individual elements in the texture. In global models, spatial resolution and localization of individual texture elements are poor, and discrimination depends on the amount of overlap between the chromatic distributions (as could be formalized by the Mahalanobis distance). Both types of conceptual models make fundamentally different predictions about how the chromatic distribution in a chromatic texture influences discrimination. In local models, two textures could be discriminated if two matching local patches are sufficiently different, no matter how different all other patches in the stimulus are and how the chromaticities of these patches are distributed. Consequently, for local models, the chromatic distribution, which is a global property, does not affect discrimination. Note that a spatial blurring as often used in local models does not take the distribution into account, as it only shifts the response toward the mean of the distribution. In global models, on the other hand, two textures can be discriminated when the two distributions are sufficiently different, that is, when there are many colors in the comparison stimulus that are not present in the test stimulus. Likewise, global models predict that two textures cannot be discriminated if the individual patches are drawn from largely overlapping chromatic distributions, even if the chromatic contrast between any two matching patches is the same above discrimination threshold. The results of this study provide evidence for a global model: Observers cannot match individual spatial locations of, for example, the test banana to the comparison banana. Instead the measured threshold elevation depends on the chromatic distribution and is largest along the direction of maximal chromatic variation, as predicted by global models.

The global model can be detailed in terms of responses of a set of higher order mechanisms to the stimulus. For illustration, consider the response of a set of higher order mechanisms to a comparison banana which is shifted by the same amount  $\delta$  either along or orthogonal to the direction of maximal chromatic variation (Figure 11). The distribution of responses for the mechanism tuned to the “banana direction” will have a mean  $\mu$  and standard deviation sigma  $\sigma$ , and the distribution of the responses to

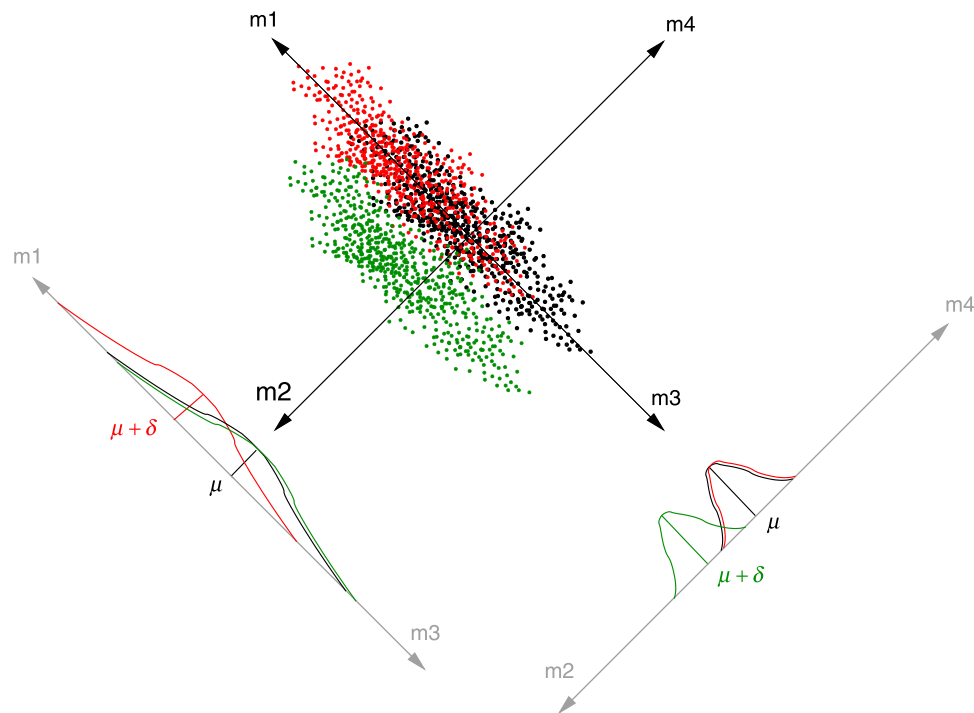


Figure 11. Response of a chromatic discrimination model with multiple mechanisms to different chromatic distributions. The model has a number of mechanisms centered at the adaptation point and tuned to different chromatic directions. For display purposes, only four of these mechanisms are shown (m1–m4). Colored point clouds sketch the chromatic distribution of a stimulus at the adaptation point (test location)  $\mu$  (black) and the distributions of two comparison stimuli that are shifted by the same amount  $\delta$  either along the direction of largest chromatic variation (red) or minimal chromatic variation (green). Gaussian-shaped curves sketch for each mechanism the distribution of responses; the responses have been displaced for better visualization (gray lines). The stimulus shifted along the axis of maximal chromatic variation cannot be discriminated because the responses have a large overlap (red). The stimulus displaced along the direction of minimal chromatic by the same amount  $\delta$  can be discriminated from the test distribution because the responses have only a small overlap.

the comparison banana will have a mean  $\mu + \sigma$  and standard deviation  $\sigma$ . When the comparison banana changes along the “banana axis”, most of these responses will overlap and the only responses that will be informative for discrimination are those produced by the colors at the end of the distribution (i.e., those color responses greater  $\mu + \delta + c\sigma$  than with criterion  $c$ ). This will not occur when the comparison banana is shifted along a different line, where it can strongly activate an orthogonal mechanism. Our long-term goal is to develop a computational model based on these ideas and to establish a full spatiotemporal line element of color space (Noorlander & Koenderink, 1983).

## Conclusion

Overall, we conclude that the distribution of chromaticities in natural objects leads to a specific increase in discrimination thresholds along the direction of maximal chromatic variation. These findings may have to be

considered when defining industrial norms for tolerable chromatic differences for any real object. They may also help to aid our understanding of other aspects of the visual processing of natural scenes.

## Acknowledgments

This research was supported by the German Science Foundation grant Ge 879/5. We are grateful to Lindsay T. Sharpe for comments on an earlier version of this manuscript. We would like to thank Constanze Hesse, Maria Olkkonen, and Diana Pittig for patiently acting as observers in these lengthy experiments.

Commercial relationships: none.

Corresponding author: Thorsten Hansen.

Email: Thorsten.Hansen@psychol.uni-giessen.de.

Address: Justus-Liebig-Universität Giessen, Abteilung Allgemeine Psychologie, Otto-Behagel-Str. 10F, 35394 Giessen, Germany.

## References

- Alder, C. (1981). A Monte Carlo method for the validation of discrimination ellipse data. *Journal of the Society of Dyers and Colourists*, 97, 514–517.
- Bergen, J. R., & Adelson, E. H. (1988). Early vision and texture perception. *Nature*, 333, 363–364. [[PubMed](#)]
- Bergen, J. R., & Landy, M. S. (1991). Computational modeling of visual texture segregation. In M. S. Landy, & J. A. Movshon (Eds.), *Computational models of visual processing*. Cambridge, MA: MIT Press.
- Boynton, R. M., & Kambe, N. (1980). Chromatic difference steps of moderate size measured along theoretically critical axes. *Color Research and Application*, 5, 13–23.
- Brown, W. R. (1957). Color discrimination of twelve observers. *Journal of the Optical Society of America*, 47, 137–143. [[PubMed](#)]
- Brown, W. R., & MacAdam, D. L. (1949). Visual sensitivities to combined chromaticity and luminance differences. *Journal of the Optical Society of America*, 39, 808–834.
- Carney, T., Klein, S. A., Tyler, C. W., Silverstein, A. D., Beutter, B., Levi, D., et al. (1999). The development of an image/threshold database for designing and testing human vision models. In B. Rogowitz, & T. Pappas (Eds.), *Human vision, visual processing, and digital display IV* (vol. 3644, pp. 542–551). Bellingham, WA: SPIE.
- Carney, T., Tyler, C. W., Watson, A. B., Makous, W., Beutter, B., Chen, C.-C., et al. (2000). ModelFest: Year one results and plans for future years. In B. Rogowitz, & T. Pappas (Eds.), *Human vision, visual processing, and digital display V* (vol. 3959, pp. 140–151). Bellingham, WA: SPIE.
- Chen, C.-C., Foley, J. M., & Brainard, D. H. (2000). Detection of chromoluminance patterns on chromoluminance pedestals II: Model. *Vision Research*, 40, 789–803. [[PubMed](#)]
- Chen, C.-C., & Tyler, C. W. (2000). ModelFest: Imaging the underlying channel structure. In B. Rogowitz, & T. Pappas (Eds.), *Human vision, visual processing, and digital display V* (vol. 3959, pp. 152–159). Bellingham, WA: SPIE.
- CIE (1978). *Recommendations on uniform color spaces, color-difference equations, psychometric color terms*. Supplement No. 2 of CIE Publ. No. 15 (E-1.3.1) 1971, Bureau Central de la CIE, Paris, 1978.
- CIE (1998). *The CIE 1997 Interim Colour Appearance Model (Simple Version)*, CIECAM97s (Publication 116–198). Paris: Bureau Central de la CIE.
- CIE (2004). *A Colour Appearance Model for Colour Management Systems: CIECAM02* (Publication 159). Paris: Bureau Central de la CIE.
- Daly, S. (1993). The visible difference predictor: An algorithm for the assessment of image fidelity. In A. B. Watson (Ed.), *Digital images and human vision* (pp. 179–206). Cambridge, MA: MIT Press.
- Derrington, A. M., Krauskopf, J., & Lennie, P. (1984). Chromatic mechanisms in lateral geniculate nucleus of macaque. *The Journal of Physiology*, 357, 241–265. [[PubMed](#)] [[Article](#)]
- D’Zmura, M., & Knoblauch, K. (1998). Spectral bandwidth for the detection of color. *Vision Research*, 38, 3117–3128. [[PubMed](#)]
- Fairchild, M. D. (1998). *Color appearance models*. Reading, MA: Addison-Wesley.
- Field, D. J. (1987). Relations between the statistics of natural images and the response properties of cortical cells. *Journal of the Optical Society of America A, Optics and image science*, 4, 2379–2394. [[PubMed](#)]
- Gegenfurtner, K. R., & Kiper, D. C. (1992). Contrast detection in luminance and chromatic noise. *Journal of the Optical Society of America A, Optics and image science*, 9, 1880–1888. [[PubMed](#)]
- Goda, N., & Fujii, M. (2001). Sensitivity to modulation of color distribution in multicolored textures. *Vision Research*, 41, 2475–2485. [[PubMed](#)]
- Godlove, I. H. (1952). Near-circular Adams chromaticity diagrams. *Journal of the Optical Society of America*, 42, 204–212.
- Halíř R., & Flusser J. (1998). Numerically stable direct least squares fitting of ellipses. In *Proceedings of the 6th International Conference in Central Europe on Computer Graphics and Visualization* (pp. 125–132). WSCG ’98. CZ, Plzeň.
- Hansen, T., & Gegenfurtner, K. R. (2006). Higher level chromatic mechanisms for image segmentation. *Journal of Vision*, 6(3):5, 239–259, <http://journalofvision.org/6/3/5/>, doi:10.1167/6.3.5. [[PubMed](#)] [[Article](#)]
- Hansen, T., Olkkonen, M., Walter, S., & Gegenfurtner, K. R. (2006). Memory modulates color appearance. *Nature Neuroscience*, 9, 1367–1368. [[PubMed](#)]
- Hillis, J. M., & Brainard, D. H. (2005). Do common mechanisms of adaptation mediate color discrimination and appearance? Uniform backgrounds. *Journal of the Optical Society of America A, Optics, image science, and vision*, 22, 2090–2106. [[PubMed](#)] [[Article](#)]
- Huertas, R., Melgosa, M., & Oleari, C. (2006). Performance of a color-difference formula based on OSA-UCS space using small–medium color differences. *Journal of the Optical Society of America A, Optics, image science, and vision*, 23, 2077–2084. [[PubMed](#)]

- Judd, D. B. (1951). Report of U. S. secretariat committee on colorimetry and artificial daylight. In *Proceedings of the Twelfth Session of the CIE, Stockholm*. Paris: Bureau Central de la CIE.
- Kawamoto, K., Inamura, T., & Shioiri, S. (2003). Color discrimination characteristics depending on the background color in the (L, M) plane of a cone space. *Optical Review*, *10*, 391–397.
- Kiener, S. (1997). On the relationship between two types of effects caused by color adaptation: Changes in color appearance and color discriminability. *Journal of Mathematical Psychology*, *41*, 107–121.
- Klein, S. A. (1993). Image quality and image compression: A psychophysicist's viewpoint. In A. B. Watson (Ed.), *Digital images and human vision* (pp. 73–88). Cambridge, MA: MIT Press.
- Krauskopf, J., & Gegenfurtner, K. (1992). Color discrimination and adaptation. *Vision Research*, *32*, 2165–2175. [[PubMed](#)]
- Krauskopf, J., Williams, D. R., & Heeley, D. W. (1982). Cardinal directions of color space. *Vision Research*, *22*, 1123–1131. [[PubMed](#)]
- Li, A., & Lennie, P. (1997). Mechanisms underlying segmentation of colored textures. *Vision Research*, *37*, 83–97. [[PubMed](#)]
- Loomis, J. M., & Berger, T. (1979). Effects of chromatic adaptation on color discrimination and color appearance. *Vision Research*, *19*, 891–901. [[PubMed](#)]
- Lovell, P. G., Párraga, C. A., Troscianko, T., Ripamonti, C., & Tolhurst, D. J. (2006). Evaluation of a multiscale color model for visual difference prediction. *ACM Transactions on Applied Perception*, *3*, 155–178.
- Luo, M. R., Cui, G., & Li, C. (2006). Uniform colour spaces based on CIECAM02 colour appearance model. *Color Research and Application*, *31*, 320–330.
- MacAdam, D. L. (1942). Visual sensitivities to color differences in daylight. *Journal of the Optical Society of America*, *32*, 247–274.
- MacAdam, D. L. (1944). On the geometry of color space. *Journal of the Franklin Institute*, *238*, 195–210.
- MacLeod, D. I., & Boynton, R. M. (1979). Chromaticity diagram showing cone excitation by stimuli of equal luminance. *Journal of the Optical Society of America*, *69*, 1183–1186. [[PubMed](#)]
- Miyahara, E., Smith, V. C., & Pokorny, J. (1993). How surround affect chromaticity discrimination. *Journal of the Optical Society of America A, Optics and image science*, *69*, 1183–1186. [[PubMed](#)]
- Moon, P., & Spencer, D. E. (1943). Metric for color space. *Journal of the Optical Society of America*, *33*, 260–269.
- Moroney, N., Fairchild, M. D., Hunt, R. W. G., Li, C., Luo, M. R., & Newmann, T. (2002). The CIECAM02 Color Appearance Model. In *Proceedings of the Tenth Color Imaging Conference: Color Science, Systems and Applications* (pp. 23–27).
- Neumann, D., & Gegenfurtner, K. R. (2006). Image retrieval and perceptual similarity. *ACM Transactions on Applied Perception*, *3*, 31–47.
- Newhall, S. M., Nickerson D., & Judd D. B. (1943). Final report of the O. S. A. subcommittee on spacing of the Munsell colors. *Journal of the Optical Society of America*, *33*, 385–418.
- Noorlander, C., & Koenderink, J. J. (1983). Spatial and temporal discrimination ellipsoids in color space. *Journal of the Optical Society of America*, *73*, 1533–1543. [[PubMed](#)]
- Poirson, A. B., Wandell, B. A., Varner, D. C., & Brainard, D. H. (1990). Surface characterizations of color thresholds. *Journal of the Optical Society of America A, Optics and image science*, *7*, 783–789. [[PubMed](#)]
- Rinner, O., & Gegenfurtner, K. R. (2000). Time course of chromatic adaptation for color appearance and discrimination. *Vision Research*, *40*, 1813–1826. [[PubMed](#)]
- Sachtler, W. L., & Zaidi, Q. (1992). Chromatic and luminance signals in visual memory. *Journal of the Optical Society of America A, Optics and image science*, *9*, 877–894. [[PubMed](#)]
- Saunderson, J. L., & Milner, B. I. (1944). Further study of omega space. *Journal of the Optical Society of America*, *34*, 167–173.
- Saunderson, J. L., & Milner, B. I. (1946). Modified chromatic value space. *Journal of the Optical Society of America*, *36*, 36–42.
- Schrödinger, E. (1920). Grundlinien einer Theorie der Farbenmetrik im Tagessehen. *Annalen der Physik*, *4*, 397–426.
- Shapiro, A. G., Beere, J. L., & Zaidi, Q. (2001). Time course of adaptation along the RG cardinal axis. *Color Research and Application*, *26*, 43–47.
- Shapiro, A. G., Beere, J. L., & Zaidi, Q. (2003). Time-course of S-cone system adaptation to simple and complex fields. *Vision Research*, *43*, 1135–1147. [[PubMed](#)]
- Shapiro, A. G., & Zaidi, Q. (1992). The effect of prolonged temporal modulation on the differential response of color mechanisms. *Vision Research*, *32*, 2065–2075. [[PubMed](#)]
- Smith, V. C., & Pokorny, J. (1996). Color contrast under controlled chromatic adaptation reveals opponent rectification. *Vision Research*, *36*, 3087–3105. [[PubMed](#)]
- Smith, V. C., Pokorny, J., & Sun, H. (2000). Chromatic contrast discrimination: Data and prediction for

- stimuli varying in L and M cone excitation. *Color Research and Application*, 25, 105–115.
- Stiles, W. S. (1959). Colour vision: The approach through increment-threshold sensitivity. *Proceedings of the National Academy of Sciences of the United States of America*, 45, 100–114.
- Sumner, P., & Mollon, J. D. (2000). Chromaticity as a signal of ripeness in fruits taken by primates. *Journal of Experimental Biology*, 203, 1987–2000. [[PubMed](#)] [[Article](#)]
- te Pas, S. F., & Koenderink, J. J. (2004). Visual discrimination of spectral distributions. *Perception*, 33, 1483–1497. [[PubMed](#)]
- von Helmholtz, H. L. F. (1867). *Handbuch der physiologischen Optik*. Hamburg und Leipzig: Voss.
- Walls, G. L. (1942). *The vertebrate eye and its adaptive radiation*. Bloomfield Hills, MI: The Cranbrook Institute of Science.
- Watson, A. B. (2000). Visual detection of spatial contrast patterns: Evaluation of five simple models. *Optics Express*, 6, 12–33. [[PubMed](#)]
- Watson, A. B., & Ahumada, A. J., Jr. (1989). A hexagonal orthogonal-oriented pyramid as a model of images representation in visual cortex. *IEEE Transactions on Biomedical Engineering*, 36, 97–106. [[PubMed](#)]
- Watson, A. B., & Ahumada, A. J., Jr. (2005). A standard model for foveal detection of spatial contrast. *Journal of Vision*, 5(9):6, 717–740, <http://journalofvision.org/5/9/6/>, doi:10.1167/5.9.6. [[PubMed](#)] [[Article](#)]
- Watson, A. B., & Ramirez, C. (1999). *A standard observer for spatial vision based on ModelFest dataset*. Optical Society of America Annual Meeting, Digest of Technical Papers, SuC6.
- Webster, M. A., & Mollon, J. D. (1991). Changes in colour appearance following post-receptoral adaptation. *Nature*, 349, 235–238. [[PubMed](#)]
- Webster, M. A., & Mollon, J. D. (1994). The influence of contrast adaptation on color appearance. *Vision Research*, 34, 1993–2020. [[PubMed](#)]
- Webster, M. A., & Mollon, J. D. (1997). Adaptation and the color statistics of natural images. *Vision Research*, 37, 3283–3298. [[PubMed](#)]
- Wichmann, F. A., & Hill, N. J. (2001). The psychometric function: I. Fitting, sampling and goodness of fit. *Perception & Psychophysics*, 63, 1293–1313. [[PubMed](#)] [[Article](#)]
- Wilson, H. R., & Regan, D. (1984). Spatial-frequency adaptation and grating discrimination: Predictions of a line-element model. *Journal of the Optical Society of America A, Optics and image science*, 1, 1091–1096. [[PubMed](#)]
- Wright, W. D. (1941). The sensitivity of the eye to small colour differences. *Proceedings of the Physical Society of London*, 53, 93–112.
- Wyszecki, G. (1963). Proposal for a new colour-difference formula. *Journal of the Optical Society of America*, 53, 1318–1319.
- Wyszecki, G., & Fielder, G. H. (1971a). Color difference matches. *Journal of the Optical Society of America*, 61, 1501–1513. [[PubMed](#)]
- Wyszecki, G., & Fielder, G. H. (1971b). New color-matching ellipses. *Journal of the Optical Society of America*, 61, 1135–1152. [[PubMed](#)]
- Wyszecki, G., & Stiles, W. S. (1982). *Color science. Concepts and methods, quantitative data and formulae* (2nd ed.). New York: Wiley.
- Xu, H., Yaguchi, H., & Shioiri, S. (2002). Correlation between visual and colorimetric scales ranging from threshold to large color difference. *Color Research and Application*, 27, 349–359.
- Zaidi, Q., Shapiro, A., & Hood, D. (1992). The effect of adaptation on the differential sensitivity of the S-cone color system. *Vision Research*, 32, 1297–1318. [[PubMed](#)]
- Zaidi, Q., Spehar, B., & DeBonet, J. (1998). Adaptation to textured chromatic fields. *Journal of the Optical Society of America A, Optics, image science, and vision*, 15, 23–32. [[PubMed](#)]
- Zeile, A. J., Smith, V. C., & Pokorny, J. (2006). Spatial and temporal chromatic contrast: Effects on chromatic discrimination for stimuli varying in L- and M-cone excitation. *Visual Neuroscience*, 23, 495–501. [[PubMed](#)]
- Zhang, X. M., & Wandell, B. A. (1996). A spatial extension to CIELAB for digital color image reproduction. *Proceedings of the Society for Information Display*, 96, 731–734.
- Zhang, X. M., & Wandell, B. A. (1998). Color image fidelity metrics evaluated using image distortion maps. *Signal Processing*, 70, 201–214.